

Electronic supplementary information for

Room-Temperature Fabrication of a Delafossite CuCrO₂ Hole Transport Layer for Perovskite Solar Cells

Wiley A. Dunlap-Shohl,^a Trey B. Daunis,^b Xiaoming Wang,^{c,d} Jian Wang,^{b,e} Boya Zhang,^b Diego Barrera,^b Yanfa Yan,^{c,d} Julia W. P. Hsu,^b David B. Mitzi^{a,f}

^a Department of Mechanical Engineering and Materials Science, Duke University, Durham, NC, USA.

^b Department of Materials Science and Engineering, The University of Texas at Dallas, Richardson, TX, USA.

^c Department of Physics and Astronomy, The University of Toledo, Toledo, OH, USA.

^d Wright Center for Photovoltaic Innovation and Commercialization, The University of Toledo, Toledo, OH, USA.

^e Department of Chemistry, The University of Washington, Seattle, WA, USA.

^f Department of Chemistry, Duke University, Durham, NC, USA.

Disclaimer: The information, data, or work presented herein was funded in part by an agency of the United States Government. Neither the United States Government nor any agency thereof, nor any of their employees, makes any warranty, express or implied, or assumes any legal liability or responsibility for the accuracy, completeness, or usefulness of any information, apparatus, product, or process disclosed, or represents that its use would not infringe privately owned rights. Reference herein to any specific commercial product, process, or service by trade name, trademark, manufacturer, or otherwise does not necessarily constitute or imply its endorsement, recommendation, or favoring by the United States Government or any agency thereof. The views and opinions of authors expressed herein do not necessarily state or reflect those of the United States Government or any agency thereof.

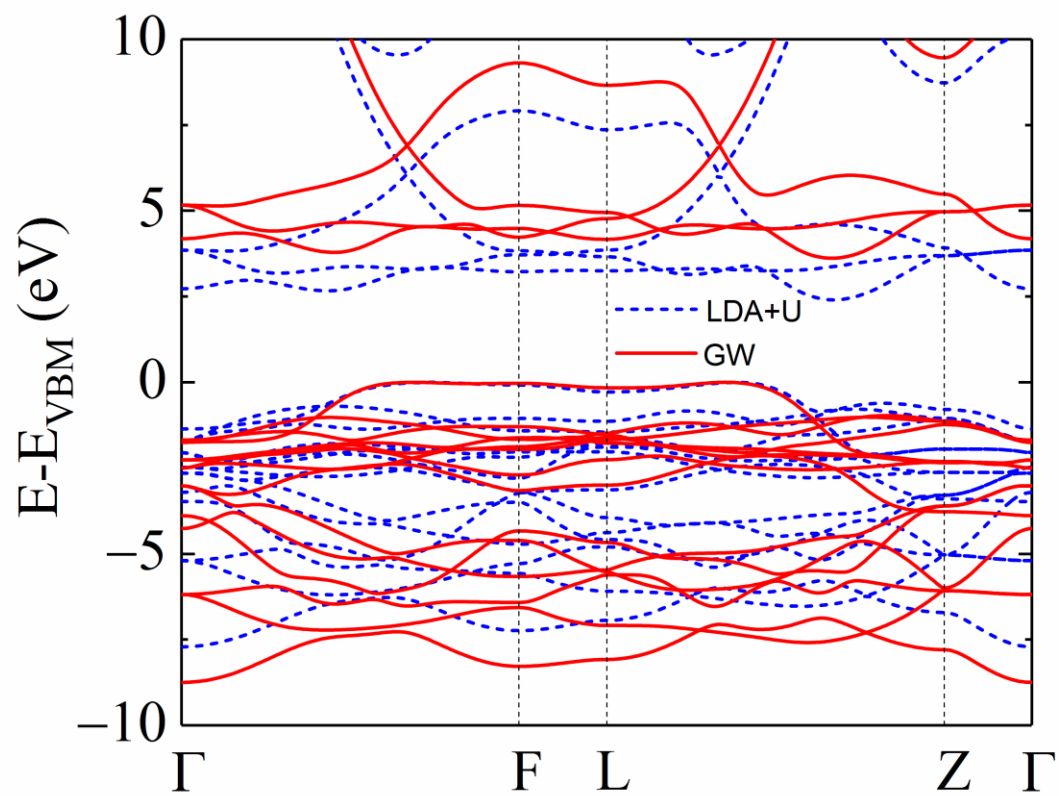


Figure S1. Comparison of the band structures of the 3R CCO in rhombohedral representation calculated by GW and LDA+U. Only the majority spin is shown for clarity.

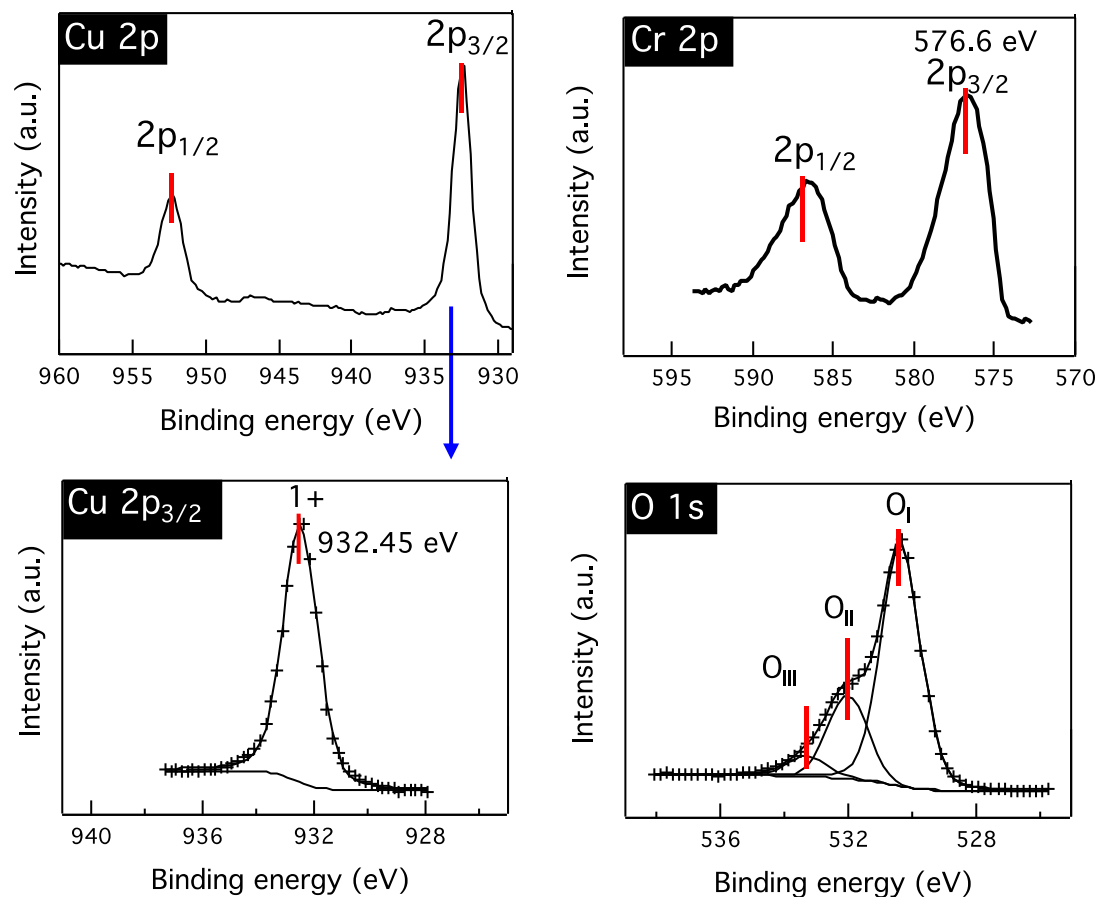


Figure S2. Region scans of X-ray photoelectron spectra of CuCrO₂ nanoparticles, demonstrating that the Cu and Cr exist only in mono- and trivalent oxidation states, in accordance with the nominal chemical formula of the material. The XPS analysis using commercial software (Multipak, Ulvac-PHI) reveals a Cu:Cr ratio of 0.9:1.

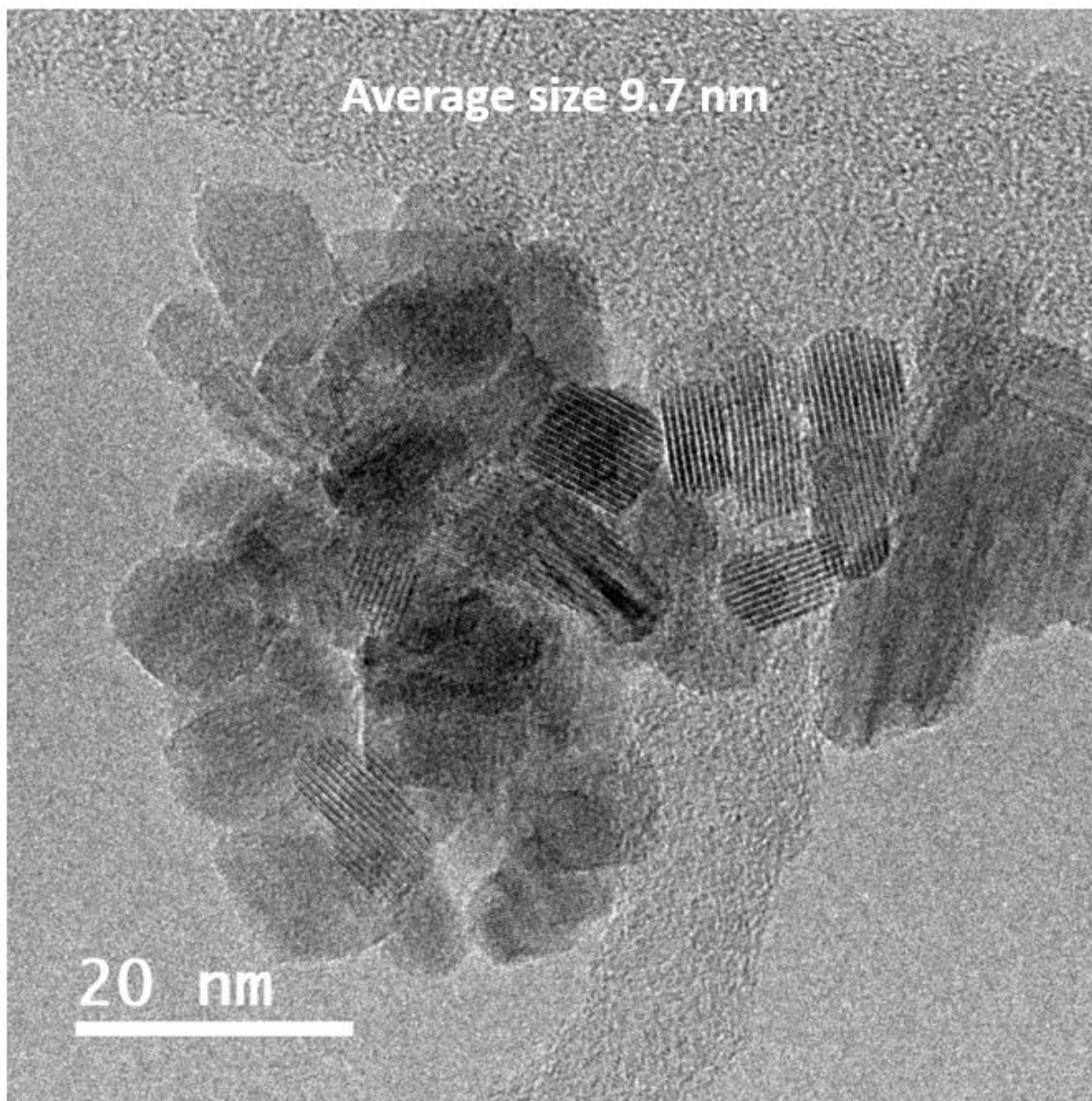


Figure S3. TEM image of CCO nanoparticles, demonstrating roughly isotropic shape and ~10 nm size.

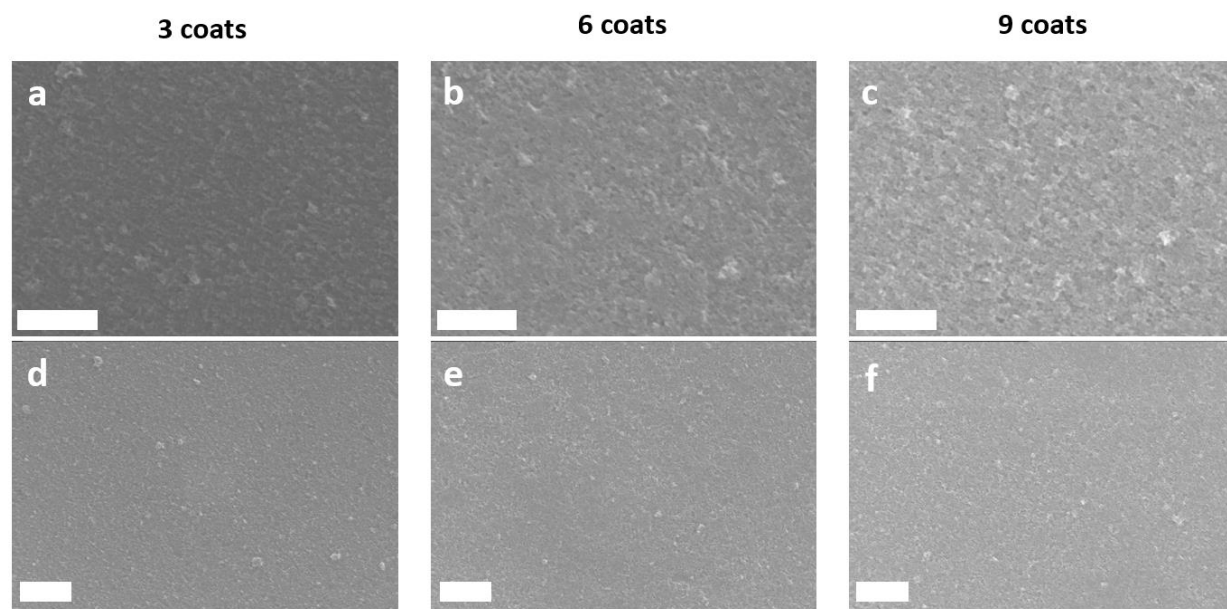


Figure S4. SEM images of CCO films on ITO, demonstrating conformal coverage of the substrate. Scale bars for high-magnification images (a-c): 500 nm; scale bars for low magnification images (d-f): 1 μm .

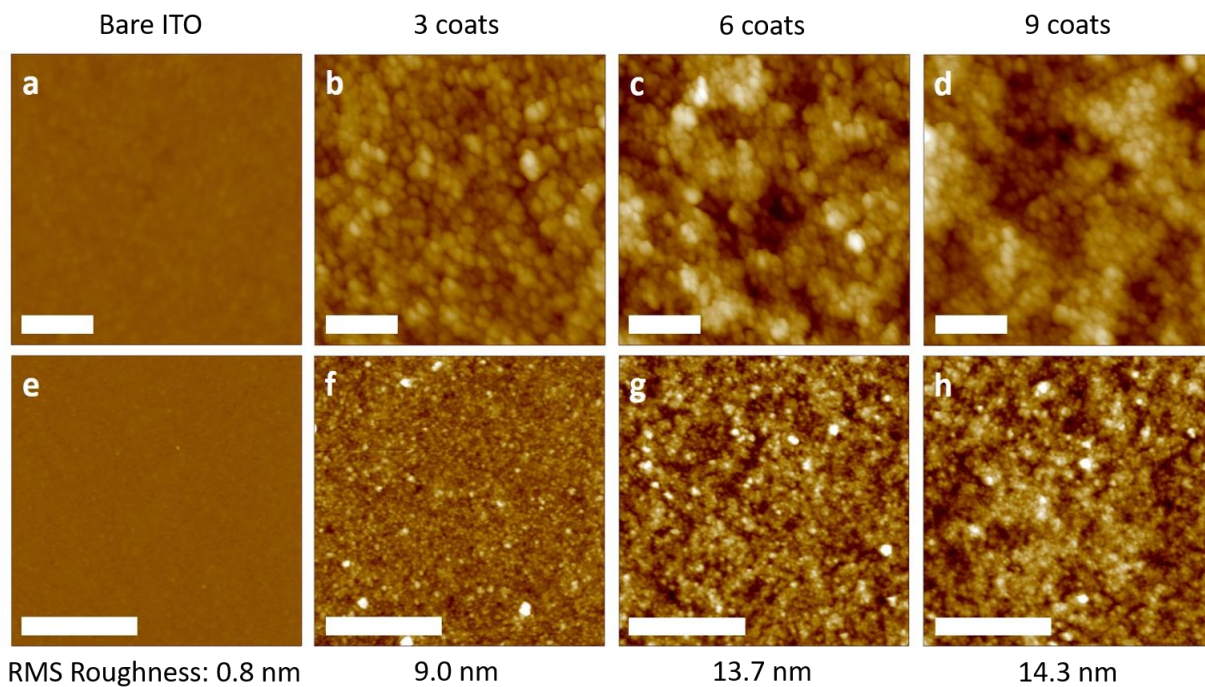


Figure S5. AFM images of CCO films on ITO along with the corresponding RMS roughness values, again demonstrating conformal coverage of the substrate. Scale bars for small area images (a-d): 250 nm; scale bars for large area images (e-h): 2 μm . Color scale for all images is 110 nm. The film RMS roughness values were calculated from 5 μm x 5 μm images.

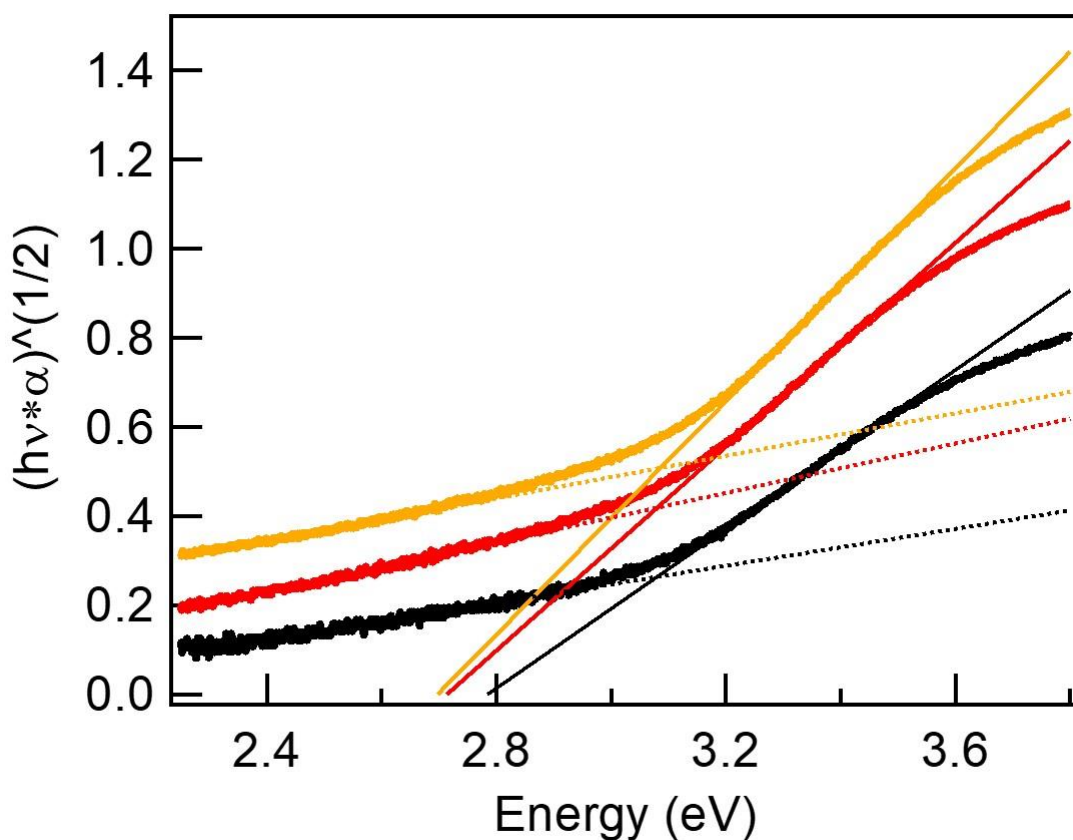


Figure S6. Tauc plots (indirect band gap) of CCO films of several thicknesses (black – 15 nm; red – 30 nm; yellow – 45 nm), showing an indirect transition at ~3.1 eV.

Table S1: Average device parameters at various CCO thicknesses from forward (reverse) J-V scans, using a measurement delay time of 1 s. Uncertainty is represented by the standard deviation of the measurements. 19, 10, 5, 13, 30, 13, and 21 devices were measured for each respective thickness, in ascending order.

CCO Thickness	V_{oc} (V)	J_{sc} (mA/cm ²)	FF (%)	PCE (%)
15 nm	0.934 ± 0.022 (0.937 ± 0.029)	20.2 ± 0.3 (20.1 ± 0.3)	57.1 ± 5.4 (56.4 ± 6.5)	10.8 ± 1.2 (10.6 ± 1.4)
17 nm	0.937 ± 0.008 (0.950 ± 0.008)	19.5 ± 0.5 (19.1 ± 0.5)	62.6 ± 1.6 (64.9 ± 1.5)	11.5 ± 0.4 (11.8 ± 0.3)
21 nm	0.963 ± 0.027 (0.975 ± 0.027)	18.8 ± 0.8 (18.6 ± 0.8)	65.6 ± 2.4 (67.1 ± 3.4)	11.8 ± 0.5 (12.1 ± 0.5)
23 nm	0.920 ± 0.010 (0.935 ± 0.017)	20.0 ± 0.3 (19.7 ± 0.2)	69.5 ± 3.1 (69.2 ± 2.9)	12.8 ± 0.6 (12.7 ± 0.6)
30 nm	0.926 ± 0.016 (0.935 ± 0.023)	19.7 ± 0.5 (19.1 ± 0.7)	65.7 ± 3.1 (67.0 ± 3.0)	12.0 ± 0.7 (12.0 ± 0.7)
33 nm	0.917 ± 0.022 (0.927 ± 0.015)	18.7 ± 0.8 (17.5 ± 1.0)	64.4 ± 2.2 (68.2 ± 1.6)	11.0 ± 0.5 (11.0 ± 0.5)
45 nm	0.928 ± 0.015 (0.932 ± 0.025)	19.0 ± 0.4 (18.2 ± 0.5)	60.2 ± 2.9 (63.2 ± 3.5)	10.6 ± 0.6 (10.7 ± 0.7)